Observation of a new dynamic recovery mechanism in the high strain regime

Yu, Tianbo; Hansen, Niels; Huang, Xiaoxu; Godfrey, Andy

Published in:
Risoe International Symposium on Materials Science. Proceedings

Publication date:
2014

Citation (APA):
Yu, T., Hansen, N., Huang, X., & Godfrey, A. (2014). Observation of a new dynamic recovery mechanism in the high strain regime. Risoe International Symposium on Materials Science. Proceedings, 35, 493-500.

OBSERVATION OF A NEW DYNAMIC RECOVERY MECHANISM IN THE HIGH STRAIN REGIME

Tianbo Yu*, Niels Hansen* Xiaoxu Huang* and Andy Godfrey**

*Danish-Chinese Center for Nanometals, Section for Materials
Science and Advanced Characterization, Department of Wind Energy,
Technical University of Denmark, Risø Campus,
Roskilde 4000, Denmark
**Key Laboratory of Advanced Materials (MoE), School of Materials
Science and Engineering, Tsinghua University,
Beijing 100084, China.

ABSTRACT

Plastic deformation of metals refines the microstructure and increases the strength through work hardening, but this effect of deformation is counterbalanced by dynamic recovery. After deformation to large strains, the microstructure typically shows a lamellar morphology, with finely spaced lamellar boundaries connected by triple junctions. Here we report that mechanically assisted triple junction motion is an important mechanism of dynamic recovery, and it replaces two boundaries by one, while maintaining the structural morphology. The observation rationalizes many features of the evolution of microstructure and strength in metals deformed to large strains, including an approach to a steady state.

1. INTRODUCTION

Metals can be shaped by deformation processes such as forging or rolling, and these processes change the metal from a soft to a hard material – a phenomenon termed work hardening or strain hardening (Friedel 1964). This hardening is caused by accumulation of defects in the form of dislocations with an increasing density as the degree of deformation is increased. However this increase of dislocation density is counterbalanced by a simultaneous dislocation removal process termed dynamic recovery (Nabarro 1989). As a result, the relative contributions of these mechanisms determine the final strength of a deformed metal. Work hardening and dynamic recovery have been studied extensively both experimentally and theoretically over the last 50 years for metals deformed to low-to-medium strains (Gil Sevillano, van Houtte and Aernoudt 1980; Kocks and Mecking 2003; Argon 2008), and mechanisms have been suggested that underpin the observed mechanical behavior. These mechanisms are based on a subdivision of the deformed structure into cells delineated by low angle dislocation boundaries. However, after deformation to high strains, the structure typically contains finely spaced extended lamellar boundaries with interconnecting boundaries and loose dislocations in between; The misorientation angle of the deformation induced boundaries can be low angle (<15°) or high angle (≥15°) (Hughes and Hansen 2000; Liu, Huang, Lloyd and Hansen 2002). In parallel to this structural evolution, the strength increases at a much slower rate than that observed at low and medium strains, indicating a shift in the balance between work hardening and softening by dynamic recovery (Hecker and Stout 1982; Godfrey and Hughes 2000). On the stress-strain curve, these changes are reflected as hardening in different stages, e.g. III and IV.

Dynamic recovery at high strains was explored by Langford and Cohen (1969), who suggested that stress or strain-induced migration of dislocation boundaries may lead to removal of cell boundaries. More recently, in a typical high strain lamellar structure, removal of lamellar boundaries via mechanically assisted triple junction motion was experimentally observed when high strain samples were further deformed (Yu, Hansen, Huang and Godfrey 2014). The new observation suggests that mechanically assisted triple junction motion is an important mechanism of dynamic recovery at high strains, which may lead to a dynamic equilibrium of structural refinement at extreme strains. In order to further understand the nature and the consequence of this important mechanism, more experimental results are reported and analyzed in the current work, following the same experimental approaches as in the previous study (Yu et al. 2014).

2. EXPERIMENTAL

The material used was commercial purity aluminum AA1050, with an initial grain size of ~100 μm and a main chemical composition of 99.5Al-0.25Fe-0.15Si (wt pct). The material was deformed by cold rolling to true strains 2, 4 and 5.5 (as-deformed state); additional cold rolling was applied to the as-deformed material (50% to strain 2 Al and 5% to strains 4 and 5.5 Al) to follow the evolution of the microstructure at high strains. The amount of additional cold rolling in thickness reduction is calculated with reference to the thickness of the as-deformed material.

Microstructural characterization was performed on the longitudinal section (containing the rolling direction RD and the normal direction ND) of the as-deformed material and over the same areas after additional cold rolling. As-deformed samples for scanning electron microscopy (SEM) analysis were mechanically polished, followed by electropolishing. SEM analyses were carried out using a Zeiss Supra-35 scanning electron microscope, equipped with a field emission gun and an Oxford Instruments HKL Channel 5 EBSD system. The microscope was operated at 15 kV for both electron channeling contrast (ECC) imaging and electron backscatter diffraction (EBSD), and for EBSD analyses step sizes of 15~30 nm were used. After additional cold rolling, the examined areas were re-examined by ECC and EBSD without further polishing of the sample surface. This process of ex situ deformation followed by re-observation can be repeated several times, following the evolution of the deformation microstructure. See Yu et al. (2014) for more experimental details.

EBSD mapping with small step sizes resulted in a contamination layer on the mapping area. The contamination layer was quite thick and could not be removed by plasma cleaning. However, this layer has a tendency to fall off during additional deformation, revealing the original polished surface (see Fig. 1a). This is a beneficial side effect of additional deformation since it improves the quality of ECC and EBSD data in subsequent observations. EBSD maps presented in the following are based on original experimental data without any post-processing to avoid introducing artifacts.

3. RESULTS

After additional deformation of the rolled aluminum, the surface roughness (both in the longitudinal and the transverse sections) is enhanced and extensive shearing is clearly observed in some places at the free surfaces. As shown in Fig. 1, the shear plane is inclined 30-40° to the RD and parallel to the transverse direction (TD). In the following, the focus will be on smooth regions without extensive shearing.

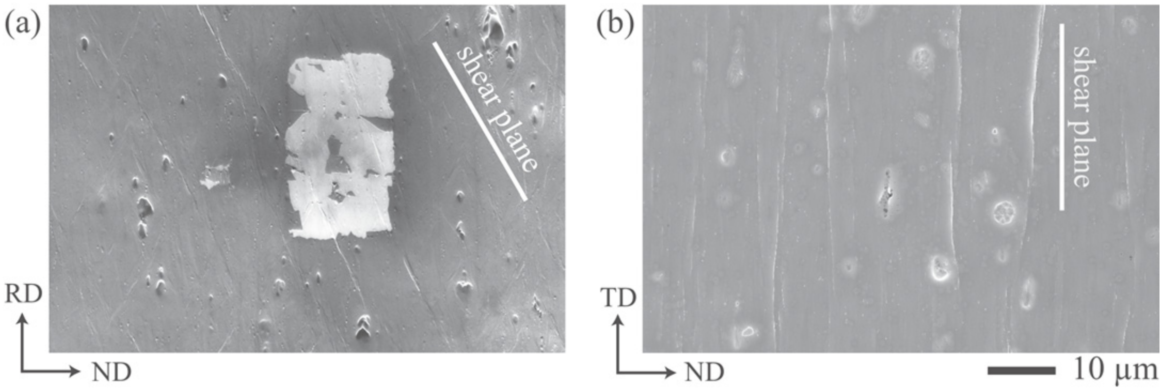

Fig. 1. SEM images show surface morphology in (a) the longitudinal section and (b) the transverse section of strain 5.5 Al after 5% additional cold rolling. The shear plane is inclined 30-40° to the RD and parallel to the TD. The rectangular white region in (a) is a result of fall-off of the EBSD-induced contamination layer during additional cold rolling.

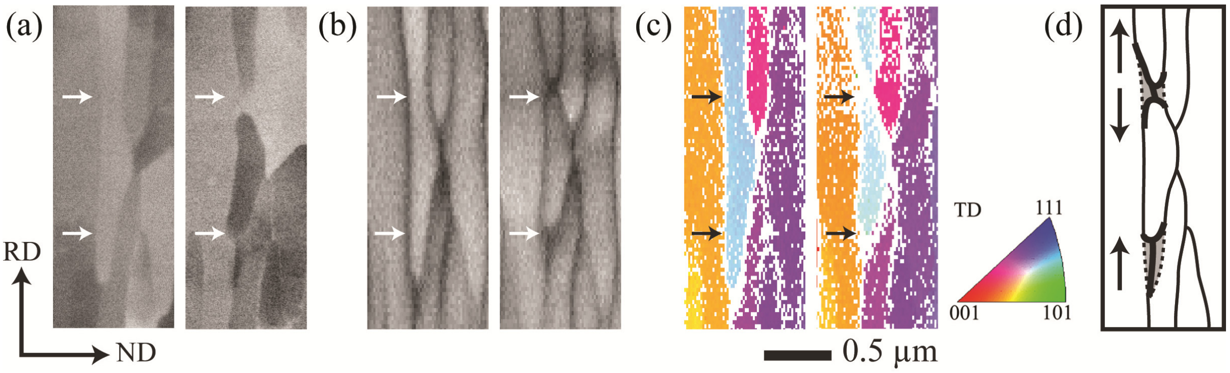

Fig. 2. (a) ECC images, (b) EBSD pattern quality maps and (c) EBSD orientation maps of the same area of strain 4 Al before (left) and after (right) 5% additional cold rolling. The color coding for the orientation maps is shown by the triangle; the white pixels correspond to not-indexed points, which were mainly distributed along lamellar boundaries; the arrows serve as references to the eyes. (d) A sketch of the evolution of the lamellar boundary structure. Solid thin lines represent lamellar boundaries that are unchanged except for geometrical compression; broken lines represent boundaries that have migrated with their new positions represented by solid bold lines. The areas swept by migrating boundaries are shown in gray, and the directions of the triple junction motion are indicated by arrows.

A comparison of the microstructure between additional rolling steps showed that the positions and misorientation angles of lamellar boundaries were almost unchanged. However, a careful comparison of individual lamella showed lateral motion of triple junctions linking the lamellar boundaries. Fig. 2 shows an example. After 5% additional cold rolling of the strain 4 Al, the triple junction at the lower tip of the arrowed lamella migrated up, as revealed simultaneously by ECC images, EBSD pattern quality (band contrast) maps and EBSD orientation maps. The migration is sketched in Fig. 2d, where the swept areas are shaded. Besides triple junction motion, the example shown in Fig. 2 also demonstrates another important phenomenon, namely break-up of lamellae. The position of break-up is indicated by upper arrows in Fig. 2a-c. The break-up of a lamella may be caused by localized shear deformation so that two neighboring lamellar boundaries meet each other (by shear banding in extreme cases). This creates a pair of triple junctions, and is typically followed by migration of the triple junction pair away from each other as sketched in Fig. 2d.

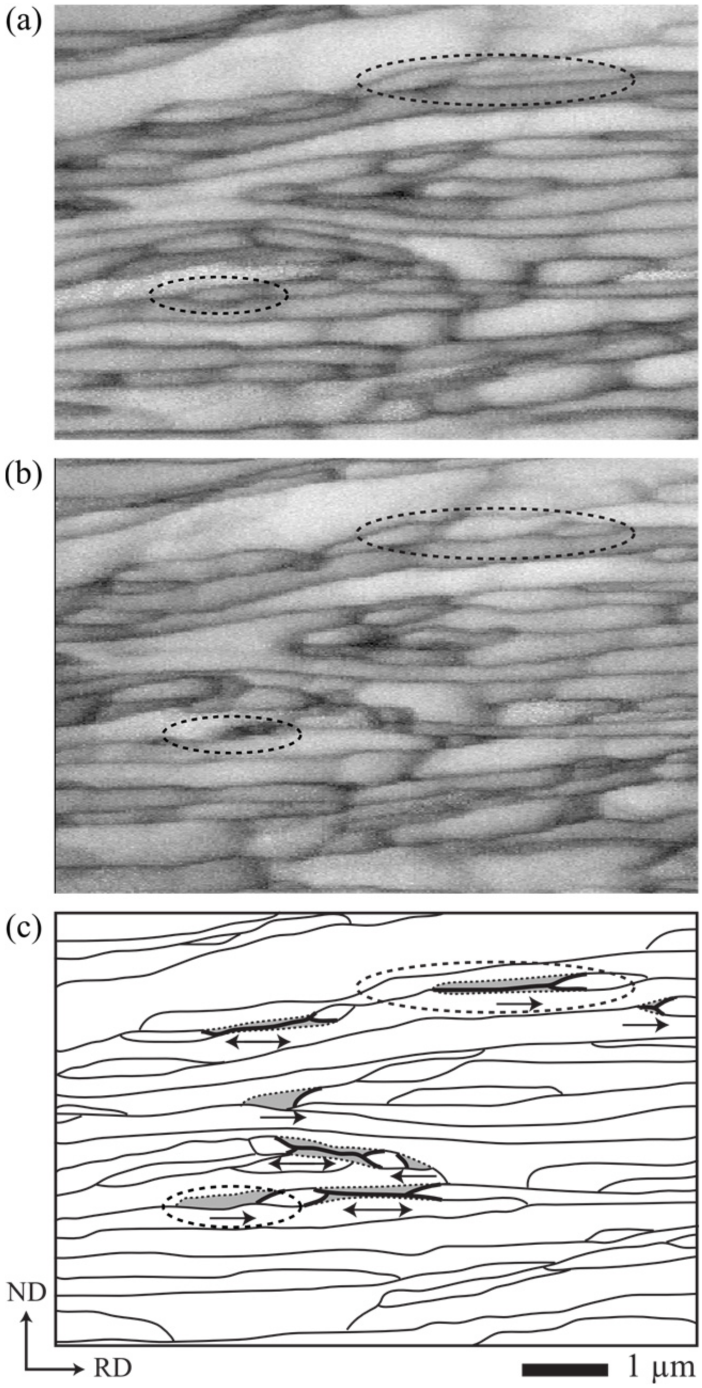

Fig. 3. (a) An EBSD pattern quality map of a selected area in the longitudinal section of strain 5.5 Al. (b) A map of the same area after 5% additional cold rolling. (c) A sketch of the evolution of the lamellar boundary structure following the same markings as in Fig. 2d. Two regions with pronounced triple junction motion are marked.

When a large area is examined before and after additional cold rolling, many cases of triple junction motion and break-up of lamellae can be observed. One example is given in Fig. 3, which shows a selected area of strain 5.5 Al before and after 5% additional cold rolling. In the corresponding sketch, double ended arrows indicate break-up of lamellae followed by migration of the newly created pairs of triple junctions, following the same mechanism illustrated in Fig. 2. The migration of a triple junction shortened one lamella and increased the boundary spacing of its two neighboring lamellae locally while keeping the general lamellar morphology. The average lamellar boundary spacing was almost unchanged due to an approximate balance between triple junction motion and geometrical reduction by the additional cold rolling.

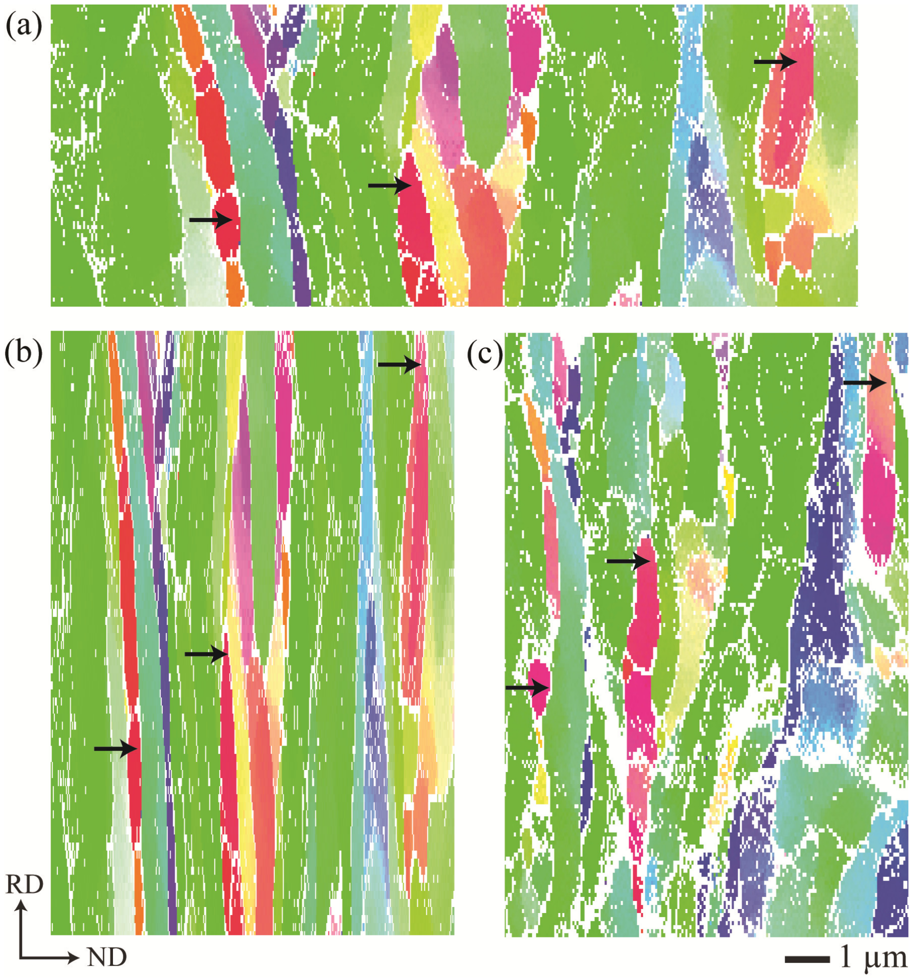

Fig. 4. (a) An EBSD orientation map of a selected area in strain 2 Al. (b) An artificial map obtained by 50% compression in the ND and 100% elongation in the RD of (a). (c) An EBSD orientation map of the same area after 50% additional cold rolling. The color coding is the same as that in Fig. 2c, and arrows indicate three reference locations in different maps.

With more additional deformation, more triple junctions migrated and over longer distances. Fig. 4 shows an example, where the microstructures of strain 2 Al before and after 50% additional cold rolling are given. Although the sample was 50% compressed in the ND and 100% elongated in the RD, the microstructure did not follow this geometrical change. As shown in Fig. 4b, the geometrical change results in highly straight lamellae with individual thickness halved. However, the real microstructure after 50% additional deformation (Fig. 4c) turns out to be very similar to the microstructure before additional deformation (Fig. 4a). The average lamellae length and thickness are only slightly changed, and the lamellar boundaries are still curved to a similar extent. In this case, many triple junctions migrated during additional deformation, and their migration played a crucial role in maintaining the structural morphology.

From analysis of the ex situ observations in all samples, triple junction motion was found typically to take place at lamellae with relatively small lamellar spacings. Besides the lamellar boundary spacing, the crystal orientations (texture) of the lamellae and the misorientation angles of the adjoining lamellar boundaries can also play a role. However, the results showed that the effect of these parameters on triple junction motion is less pronounced when compared to the lamellar boundary spacing.

4. DISCUSSION

The present observations have some similarities to those observed during annealing of highly strained aluminum, where thermally activated triple junction motion was found to be an important recovery mechanism, leading to uniform coarsening of lamellar deformed structures (Yu, Hansen and Huang 2011). However, thermally activated triple junction motion only has a marginal effect during annealing below 100 °C (Yu, Hansen and Huang 2012) and thus cannot explain the present observations, where no significant temperature increase was observed during additional cold rolling. It is therefore suggested in the previous work (Yu et al. 2014) that the observed triple junction motion during cold rolling is primarily mechanically assisted and that the mechanism can be classified as dynamic recovery, although some thermal activation will be always present. Triple junction motion replaces two lamellar boundaries by one and removes interconnecting boundaries and dislocations in swept regions, while maintaining the structural morphology. As a result, this mechanism, supplemented by break-up of lamellae, rationalizes many features of microstructural evolution at high strains, including an approach to a dynamic equilibrium (Yu et al. 2014).

The formation of a finely spaced lamellar structure is a prerequisite for triple junction motion. During deformation of a coarse grained metal, a cell block structure is typically formed after a low-to-medium strain, with extended geometrically necessary boundaries (GNBs) inclined to the rolling plane (Hansen 2001). As the strain is increased, GNBs gradually align themselves to the rolling plane, becoming lamellar boundaries. At a strain of $\varepsilon=1$, many S-shaped bands can be observed in the longitudinal section of cold rolled metals, e.g. Ni and Al (Hughes and Hansen 2000; Liu et al. 2002), indicating local shearing and a transition to a lamellar structure. At this strain, the average lamellar boundary spacing is 0.3 μm for Ni and 0.6 μm for Al. Due to the small lamellar boundary spacing achieved, mechanically assisted triple junction motion may become operative at this stage. Therefore upon further deformation, the decrease of lamellar boundary spacing becomes significantly slower than the observed geometrical reduction (Hecker and Stout 1982; Godfrey and Hughes 2000; Huang and Prangnell 2008). As shown in Fig. 4, the structural refinement after a strain of $\varepsilon=2$ is very slow. In order to further efficiently refine the microstructure and to strengthen the material by cold working, it is necessary to suppress triple junction motion by introducing pinning forces, where an example is particle pinning. More efficiently, phase boundaries may be introduced to suppress triple junction motion since their migration requires long-range diffusion of atoms, which is very difficult at low homologous temperatures, and the nanostructure and ultrahigh strength of heavily deformed pearlitic steel serves a good example (Wetscher, Pippan, Sturm, Kauffmann, Scheu and Dehm 2006; Zhang, Godfrey, Huang, Hansen and Liu 2011).

5. CONCLUDING REMARKS

The present study has shown that mechanically assisted triple junction motion is an important dynamic recovery mechanism during high strain deformation. Triple junction motion replaces two lamellar boundaries by one, and together with break-up of lamellae by localized shear deformation, rationalizes an approach to dynamic equilibrium of structural refinement at large strains. In order to further understand this mechanism and produce stronger metals and alloys by plastic deformation, in situ studies by transmission electron microscopy (TEM), as well as detailed characterization of triple junctions by high resolution TEM, are ongoing.

ACKNOWLEDGEMENTS

The authors gratefully acknowledge the support from the Danish National Research Foundation (Grant No. DNRF86-5) and the National Natural Science Foundation of China (Grant No. 51261130091) to the Danish-Chinese Center for Nanometals, within which this work has been performed.

REFERENCES

Argon, A.S. (2008). Strengthening mechanisms in crystal plasticity (Oxford University Press, Oxford).

Friedel, J. (1964). Dislocations (Pergamon, Oxford).

Godfrey, A., and Hughes, D.A. (2000). Scaling of the spacing of deformation induced dislocation boundaries. Acta Mater. 48, 1897-1905.

Gil Sevillano, J., van Houtte, P., and Aernoudt, E. (1980) Large strain work-hardening and textures. Prog. Mater. Sci. 25, 69-412.

Hansen, N. (2001). New discoveries in deformed metals. Metall. Mater. Trans. A 32, 2917-2935.

Hecker, S., and Stout, M. (1982). Strain hardening of heavily cold worked metals. In: Deformation, processing and structure. Ed. G. Krauss (American Society for Metals, Metals Park (OH)) 1–46.

Huang, Y., and Prangnell, P.B. (2008). The effect of cryogenic temperature and change in deformation mode on the limiting grain size in a severely deformed dilute aluminium alloy. Acta Mater. 56, 1619-1632.

Hughes, D.A., and Hansen, N. (2000). Microstructure and strength of nickel at large strains. Acta Mater. 48, 2985-3004.

Kocks, U.F., and Mecking, H. (2003) Physics and phenomenology of strain hardening: the FCC case. Prog. Mater. Sci. 48, 171–273.

Langford, G., and Cohen, M. (1969). Strain hardening of iron by severe plastic deformation. ASM Trans. Q. 62, 623–638.

Liu, Q., Huang, X., Lloyd, D.J., and Hansen, N. (2002). Microstructure and strength of commercial purity aluminium (AA 1200) cold-rolled to large strains. Acta Mater. 50, 3789-3802.

Nabarro, F. (1989). Work-hardening and dynamical recovery of FCC metals in multiple glide. Acta Metall. 37, 1521-1546.

Wetscher, F., Pippan, R., Sturm, S., Kauffmann, F., Scheu C., and Dehm, G. (2006). TEM investigation of structural evolution in a pearlitic steel deformed by high-pressure torsion. Metall. Mater. Trans. A 37, 1963-1968.

Yu, T., Hansen, N., and Huang, X. (2011). Recovery by triple junction motion in aluminium deformed to ultrahigh strains. Proc. R. Soc. A 467, 3039-3065.

Yu, T., Hansen, N., and Huang, X. (2012). Recovery mechanisms in nanostructured aluminium. Philos. Mag. 92, 4056–4074.

Yu, T., Hansen, N., Huang, X., and Godfrey, A. (2014). Observation of a new mechanism balancing hardening and softening in metals. Materials Research Letters 2, 160-165.

Zhang, X., Godfrey, A., Huang, X., Hansen, N., and Liu, Q. (2011). Microstructure and strengthening mechanisms in cold-drawn pearlitic steel wire. Acta Mater. 59, 3422-3430.